

Baseline Resistance Cancellation Circuit for High Resolution Thiolate-Monolayer-Protected Gold Nanoparticle Vapor Sensor Arrays

D. Rairigh, A. Mason, [†]M. P. Rowe, [†]E. T. Zellers

Michigan State Univ., East Lansing, MI, USA, [†]Univ. of Michigan, Ann Arbor, MI, USA

Abstract—Chemiresistive (CR) sensors and sensor arrays coated with thiolate-monolayer-protected gold nanoparticle (MPN) interfaces show great promise for high-sensitivity multi-vapor analysis but suffer from process variation and drift in baseline values. This paper describes a new readout circuit that cancels baseline resistance and compensates for baseline drift to achieve ppm resolution. Requiring only $5100\mu\text{m}^2$ in a $0.5\mu\text{m}$ CMOS process, the circuit is well suited for high density on-chip CR sensor arrays. The resulting CR array microsystem introduces a valuable tool for monitoring environmental hazards including explosive compounds.

I. INTRODUCTION

The demand for sensing systems capable of detecting, classifying, and quantifying volatile organic compounds, including many explosives, remains high for both civilian and military environmental monitoring applications. Chemiresistors (CR) that use thiolate-monolayer-protected gold nanoparticles (MPN) as interfacial layers have been demonstrated as highly sensitive vapor sensors, and arrays of CRs that incorporate MPNs with different thiolate ligand structures provide selective determinations of a wide range of vapors by virtue of the pattern derived from the collective responses of the sensor array [1,2]. MPN-coated CR arrays offer several advantages for multi-vapor analysis. These include facile fabrication, low-temperature operation, detection limits that are lower than other microsensors employing sorptive interface layers, differential sensitivities to a broad range of organic vapors, and favorable scaling behavior that permits miniaturization without loss of sensitivity [3]. Successful applications of MPN-coated CR arrays as detectors in meso- and micro-scale gas chromatographic instrumentation for the determination of indoor air contaminants and environmental tobacco smoke markers have been reported [1,4]. However, the accurate identification and quantification of vapors require reliable compensation for the drift in the baseline resistances of the sensors in the array. Moreover, baseline resistance compensation is necessary to fully exploit the high sensitivity of MPN-coated CR sensors.

Although MPNs are well suited for on-chip microsystem implementation, high performance integrated circuitry tailored to support these sensors has not been reported. The

resistance-to-frequency interface circuits traditionally employed with resistance-based gas sensors [5-7] work well when the sensor's response is large with respect to its base resistance. Logarithmic converters are also commonly used [8] for resistive sensors with large responses. However, these approaches lack the resolution to fully exploit the sensitivity to vapor-induced perturbations in electrical conduction inherent to MPN films. In this paper, a new readout circuit is presented that corrects for baseline variations and drift and fully utilizes the sensitivity inherent to MPN-coated CRs.

II. THIOLATE-MONOLAYER-PROTECTED GOLD NANOPARTICLE SENSORS AND SENSOR ARRAYS

MPN-coated CRs were first reported a decade ago [7]. Electrical conduction through thin MPN films occurs by electron tunneling between adjacent gold cores. Vapors can reversibly partition into the film and change the average inter-core distance as well as the dielectric constant of the organic layers separating the cores. This leads to a reversible shift in the electrical resistance of the film, which can be measured using an underlying interdigitated electrode (IDE). Changes in the baseline-normalized resistance of MPN-coated CRs are proportional to the air concentration of the vapor, and detection limits in the part-per-billion concentration range are achievable [3]. In this study, CR sensors were fabricated by patterning Cr/Au IDEs on a thick thermal oxide layer via a standard lift-off process. Each IDE consists of 20 pairs of electrodes that are $15\mu\text{m}$ wide, 1.4mm long, and spaced $15\mu\text{m}$ apart. MPN films were spray deposited from toluene solution using an air brush. Representative data for one type of MPN with a 4.3-nm -diameter gold core and a monolayer of 6-phenoxyhexane-1-thiolate (OPH) are presented below. Sensor responses are reported as the change in resistance (ΔR) divided by the baseline resistance (R_b) of the coated sensor, $\Delta R/R_b$. It has been shown that $\Delta R/R_b$ is virtually independent of the thickness of the MPN layer over the range of useful film thicknesses ($\sim 10\text{-}200\text{nm}$) [3].

III. REQUIREMENTS FOR HIGH SENSITIVITY

While the normalized resistance change ($\Delta R/R_b$) of the MPN-coated CR sensor provides very reliable results, the actual sensor response ($\Delta R + R_b$) requires some manipulation to extract the value of interest. Furthermore, the base resistance (R_b) of the sensor drifts significantly over time and requires compensation. To achieve very high resolution measurements of ΔR , it is preferable to cancel R_b in the

This work is supported by the Department of Homeland Security, Science and Technology Directorate (06-G-024).

analog domain before amplification, permitting the full range of an analog to digital converter (ADC) to focus on the ΔR output component. As illustrated in Figure 1, when the total response is digitized, the majority of the ADC's resolution is expended digitizing the base resistance, and the actual resolution used to digitize ΔR is very small. Conversely, when R_b is removed in the analog domain before the signal is digitized, high resolution measurements can be achieved.

Baseline resistance cancellation also significantly improves signal to noise ratio (SNR). If the base resistance is not removed, it will drastically limit the gain that can be applied to the signal. Thus the noise introduced in each stage will be large in proportion to the ΔR signal. Removing the baseline resistance immediately allows the actual sensor response to be amplified up to 10^6 times more, increasing the SNR of the circuit.

Assuming that the nominal R_b is $1M\Omega$, that the sensor is stimulated with a $1\mu A$ current, and that a voltage response is read out, initial specifications for the interface circuit with base cancellation can be computed. An ADC resolution of 7 bits provides $1ppm < \Delta R/R_b < 100ppm$ resolution, given perfect base cancellation. Thus, the input referred noise of the cancellation stage must be $< 1\mu V$.

IV. BASE CANCELLATION CIRCUIT

A. Circuit Architecture

The architecture for the proposed CR instrumentation circuit is shown in Figure 2. Here, the sensor is stimulated with a constant bias current, and the voltage response

$$V_{sens} = I_R (\Delta R + R_b) \quad (1)$$

is input to the base cancellation stage. The base cancellation stage removes a baseline value $I_R R_b$, previously stored in the analog memory (AM), from V_{sens} , and outputs only the actual sensor response, $I_R \Delta R$. Because this response is very small and susceptible to noise, the initial gain stages are fully differential so that common mode noise can be canceled.

B. Base Cancellation Stage

A possible base cancellation stage has been presented in [9]. The alternative presented here eliminates the need for feedback resistors or a power gain stage (required in an op-amp using feedback). This eliminates multiple noise sources as well as reduces the area and power consumption of the overall circuit. A simplified schematic of the new base cancellation system is shown in Figure 3, where the output of the sensor is read at V_{sens} and the value stored in the AM appears at V_{AM} . When V_{AM} is exactly equal to $I_R R_b$ and the differential pair is operating in the subthreshold region, the differential output voltage is

$$V_{+out} - V_{-out} = \kappa I_R \Delta R \quad (2)$$

where κ , the subthreshold gate efficiency, is close to unity. Subthreshold operation is important because it gives a significantly more linear response than operation above threshold. It also has the advantage of lower power

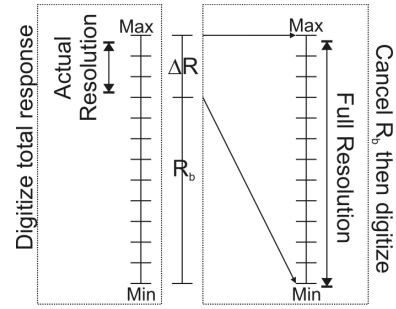


Figure 3: When the entire sensor response is digitized, ΔR receives only a small portion of the ADC's resolution. If, however, R_b is first canceled, the full resolution of the ADC may be used.

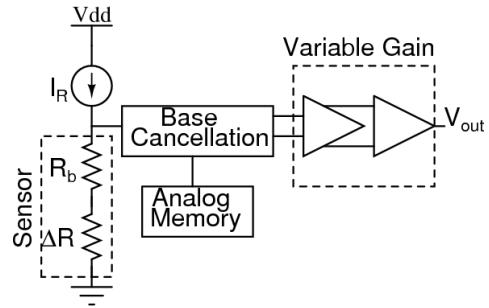


Figure 3: Baseline cancellation circuit architecture. The sensor is stimulated with a constant current, and the voltage change is read by the Base Cancellation stage that uses the value stored in the Analog Memory to remove the baseline signal. The signal is then amplified before digitization.

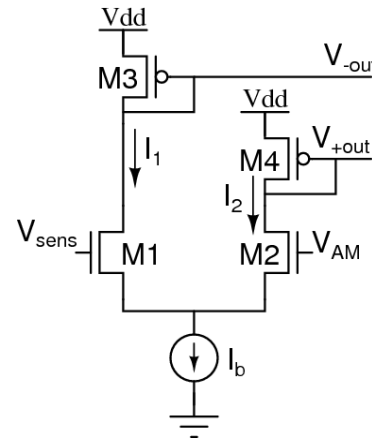


Figure 3: Simplified schematic of the base cancellation system. Sensor response is read at V_{sens} and the analog memory value at V_{AM} . Bias current I_b is set to ensure that the circuit operates in the subthreshold region.

consumption, which becomes a requirement when many of these interface circuits are replicated on a chip to support a large array of chemiresistors [10].

Within the base cancellation stage, signal levels are on the order of micro-volts, and limiting noise is critical. By maintaining a differential signal at the output, the common

mode noise, including noise from I_b , can be canceled. To further reduce noise, M1-M4 in Figure 3 should be sized carefully in a tradeoff of conflicting size requirements for improving linearity.

C. Analog Memory

To set the baseline cancellation value in the AM, a very simple calibration routine is used. When the sensor is not responding ($\Delta R=0$), the readout circuit output should be 0V. During calibration, a feedback loop from the variable gain amplifier output to the AM is used to drive the output to 0. Once this state is achieved, calibration is complete and the AM will hold the proper baseline cancellation value. This approach also has the advantage of compensating for all non-ideal offsets in the base cancellation and gain stages. Furthermore, the feedback approach allows for rapid calibration; convergence is limited only by the speed of the AM. Relatively rapid convergence is necessary because the drift of CR baseline values (R_b) can be significant, and the system must be recalibrated as frequently as possible.

If the time between recalibration periods were short enough, a capacitor-based AM could be used to store a purely analog value and provide exact cancellation. However, the readout cycle of CR sensors, and thus the time between calibrations, is on the order of seconds, and charge leakage disallows the use of a capacitor-based AM. Therefore, the AM has been implemented with a digital to analog converter (DAC), which can hold its value indefinitely. Notice that after a calibration cycle, the DAC holds the value of the baseline resistance. Thus, an added advantage of the DAC approach is having the baseline resistance (R_b) readily available as an output.

The disadvantage of a DAC-based AM is that the exact value of base resistance can not be stored. Instead the DAC stores

$$V_{AM} = I_R R_b' \quad (3)$$

where R_b' is within one LSB of the actual R_b . To determine the necessary resolution of the DAC, consider that the baseline cancellation error can be expressed by

$$\varepsilon = I_R (R_b - R_b') \leq \frac{V_{max} - V_{min}}{2^N} \quad (4)$$

where V_{max} to V_{min} is the output range of the DAC and N is the number of bits of resolution of the DAC. Clearly, limiting the output range will reduce error, so the minimum output range must first be determined. For the CR sensors targeted by this system, R_b is expected to vary from $1M\Omega$ to $10M\Omega$. To support a wide range of possible R_b values, I_R must be variable. In this circuit, I_R has been set to vary from 75nA to 525nA. To match this, the DAC output range has been chosen as 0.5V to 1V. Given this range, (4) shows that a 9-bit DAC limits the output error to less than 1mV, which is well within the total system's linear range. Although the DAC needs to support relatively high resolution, this application has no practically challenging requirements on linearity or speed. DAC resolution requirements could be reduced by increasing

the range of I_R , which would permit a smaller output range for the DAC.

D. Variable Gain Stage

The differential output of the base cancellation stage is passed through a variable gain amplifier. This provides the option to “zoom in” on a very small sensor response or “zoom out” and provide a wide dynamic range. This variable gain is necessary to support the wide range of sensor output sensitivities, $1\text{ppm} < \Delta R/R_b < 100\text{ppm}$, for the target sensors.

V. TEST RESULTS

To measure a sensor's response, both the ΔR and R_b must be tracked accurately. Figure 4, shows the very dramatic drift in R_b in a CR sensor element coated with a film of OPH-MPNs. This demonstrates the need for baseline tracking. The inset in Figure 4 illustrates the normalized sensor response.

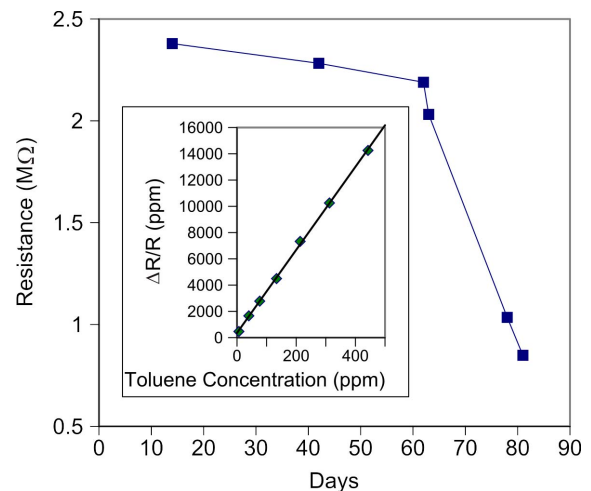


Figure 4: Drift in R_b over time for the OPH-MPN coated CR. Inset shows a toluene vapor calibration curve for a CR coated with a $\sim 180\text{-nm}$ film of OPH-MPN ($r^2 = 0.997$).

The new CR readout circuit was fabricated in a $0.5\mu\text{m}$ CMOS process. The differential pair and differential gain stage (excluding the second variable gain portion) together occupy $116\mu\text{m} \times 44\mu\text{m}$ (Figure 5). For testing, a data acquisition card was used to provide the analog memory and DAC functions of the overall instrument. The on-chip current bias proved to be excessively noisy, so an external voltage source was used to model the behavior of a biased sensor. Figure 6 shows test results for a modeled $I_R R_b$ of 2V. This data was read from the differential gain stage and digitally low pass filtered. This demonstrates an initial resolution of approximately 10ppm. In contrast, a recently published resistance-to-frequency system reported a precision of only 0.4% or 4000 ppm over 4 decades of total resistance variation [5]. Because of the base cancellation, the new circuit presented here provides over two decades more resolution, although the current version does not include digital conversion.

The new system also has significant dynamic range. It

can read a sensor response, $I_R \Delta R$, of up to $\pm 25\text{mV}$. For a $2\text{M}\Omega$ base resistance biased at 1V , this equates to a ΔR of $\pm 50\text{k}\Omega$. The bias generator for I_R in this system can also accommodate a base resistance, R_b , ranging from $2.7\text{M}\Omega - 18\text{M}\Omega$.

Figure 7 demonstrates the baseline tracking ability of this system. Plot (a) shows the model sensor output voltage and plot (b) shows the output of the CR readout circuit. Both sensor responses and baseline drift are modeled here, but only the baseline drift is apparent from directly measuring the

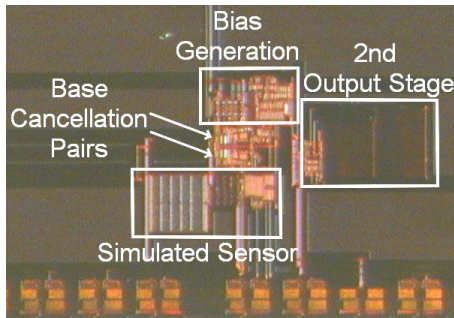


Figure 7: Chip photograph of base cancellation system.

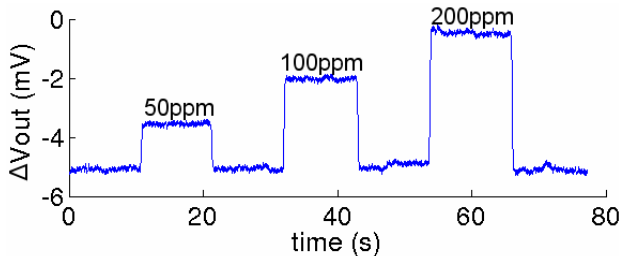


Figure 7: Filtered output of CR readout circuit for small sensor responses. The baseline, $I_R R_b$, for this test was approximately 2V .

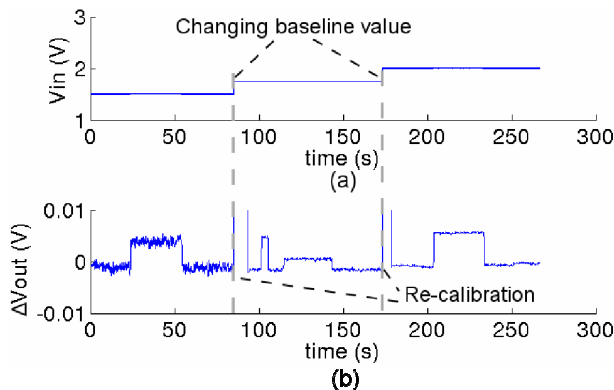


Figure 7: Demonstration of baseline tracking. (a) Model sensor output at three typical baseline resistance values. Note that the sensor response is swamped by baseline drift. (b) Output of CR readout circuit that removes the baseline and allows sensor response to be measured.

sensor voltage; the sensor response is too small to be detected. However, in Figure 7b, the readout circuit output clearly shows each sensor response as the circuit calibrates for each new baseline value. This demonstrates baseline tracking as well as the necessity for baseline cancellation.

VI. CONCLUSION

MPN-coated CR sensors and sensor arrays provide high sensitivity vapor sensors, with many applications in environmental monitoring. These sensors are capable of achieving detection limits in the part-per-billion vapor concentration range. To make full use of these sensors, a new instrumentation circuit capable of tracking and canceling the baseline resistance was presented. The circuit features a unique differential baseline cancellation analog block that operates in the subthreshold region, as well as a low noise output stage. Fabricated in a $0.5\mu\text{m}$ CMOS process, the core component dimensions are $116\mu\text{m} \times 44\mu\text{m}$, making it highly suitable for high density on-chip CR sensor arrays. Measurements show the circuit has resolution sufficient to read a relative resistance change of approximately 10 ppm, and tradeoffs in circuit design permit resolution to be increased in future iterations. Good tracking of drifting baseline values through a calibration procedure has also been experimentally verified.

REFERENCES

- [1] C. Lu, W. H. Steinecker, W. Tian, M. C. Oborny, J. M. Nichols, M. Agah, J. A. Potkay, H. K. L. Chan, J. Driscoll, R. D. Sacks, K. D. Wise, S. W. Pang, E. T. Zellers, "First-generation hybrid MEMS gas chromatograph," *Lab on a Chip*, vol. 10, pp. 1123-1131, 2005.
- [2] L. Han, X. Shi, W. Wu, F. L. Kirk, J. Luo, L. Wang, D. Mott, L. Cousineau, S. I. Lim, S. Lu, C. Zhong, "Nanoparticle-structured sensing array materials and pattern recognition for VOC detection," *Sens. Actuators, B.*, vol. 106, pp. 431-441, 2005.
- [3] W. H. Steinecker, M. P. Rowe, E. T. Zellers, "Model of vapor-induced resistivity changes in gold-thiolate monolayer-protected nanoparticle sensor films," *Anal. Chem.*, vol. 79, pp. 4977-4986, 2007.
- [4] Q. Zhong, R. A. Veeneman, W. H. Steinecker, C. Jia, S. A. Batterman, E. T. Zellers, "Rapid determination of ETS markers with a prototype field-portable GC employing a microsensor array detector," *J. Environmental Monitoring*, vol. 9, no. 5, pp. 440-448, 2007.
- [5] M. Grassi, P. Malcovati, A. Baschiroto, "A 141-dB dynamic range CMOS gas-sensor interface circuit without calibration with 16-bit digital output word," *IEEE J. Solid-State Circuits*, vol. 42, no. 7, pp. 1543-1554, Jul 2007.
- [6] A. Flammini, D. Marioli, A. Taroni, "A low-cost interface to high-value resistive sensors varying over a wide range," *IEEE Trans. Instrumentation and Measurement*, vol. 53, no. 4, pp. 1052-1056, Aug 2004.
- [7] H. Wohltjen, A. W. Snow, "Colloidal metal-insulator-metal ensemble chemiresistor sensor," *Anal. Chem.*, vol. 70, pp. 2856-2859, 1998.
- [8] D. Barlettino, M. Graf, S. Taschini, S. Hafizovic, C. Hagleitner, A. Hierlemann, "CMOS monolithic metal-oxide gas sensor microsystems," *Sensors Journal*, IEEE, vol. 6, no. 2, pp. 276-286, Apr 2006.
- [9] T. J. Koickal, A. Hamilton, S. Tan, J. Covington, J. Gardner, T. Pearce, "Smart interface circuit to ameliorate loss of measurement range in chemical microsensor arrays," *Proc. IEEE Instrumentation and Measurement Technology*, vol. 1, pp. 548-550, May 2005.
- [10] J. Covington, S. Tan, J. Gardner, A. Hamilton, T. Koickal, T. Pearce, "Combined smart chemFET/resistive sensor array," *IEEE Sensors*, vol. 2, pp. 1120-1123, Oct 2003.